Wallis, G. B., *One-Dimensional Two-Phase Flow*, pp. 175-281, McGraw-Hill, N.Y. (1969).
Wallis, G. B., "The Terminal Speed of Single Drops or Bubbles in an Infinite Medium," *Int. J. Multiphase Flow*, **1**, 491 (1974).
Weaver, R. E. C., L. Lapidus, and J. C. Elgin, "The Mechanics of Vertical Moving Liquid-liquid Systems I," *AIChE J.*, **5**, 533 (1959).
Wen, C. Y. and Y. H. Yu, "Mechanics of Fluidization," *Chem. Eng. Prog. Sym. Series, Fluid Particle Technology*, **62** (62), 100 (1966).
Werther, J., "Influence of the Bed Diameter on the Hydrodynamics of Gas Fluidized Beds," *AIChE Sym. Series*, **70** (141), 53 (1974).
Yoshida, F., and Akita, K., "Performance of Gas Bubble Columns: Volumetric Liquid-Phase Mass Transfer Coefficient and Gas Holdup," *AIChE J.*, **11**, 9 (1965).
Zenz, F. A., and D. F. Othmer, *Fluidization and Fluid Particle Systems*, Reinhold, N.Y. (1960).
Zuber, N., "On the Dispersed Two-Phase Flow in the Laminar Flow Regime," *Chem. Eng. Sci.*, **19**, 897 (1964).
Zuber, N., "Flow Excursions and Oscillations in Boiling, Two-Phase Flow Systems with Heat Addition," Proceedings of Sym. of Two-Phase Flow Dynamics, **1**, 1071 (1967).
Zuber, N. and J. Hench, "Steady State and Transient Void Fraction of Bubbling Systems and Their Operating Limits," General Electric Co. Report No. 62GL100 (1962).
Zuber, N. and J. A. Findley, "Average Volumetric Concentration in Two-Phase Flow Systems," *J. Heat Trans.*, **87**, 453 (1965).
Zuber, N., F. W. Staub, G. Bijwaard, and P. G. Kroeger, "Steady State and Transient Void Fraction in Two-Phase Flow Systems," General Electric Co. Report GEAP-5417, Vol. 1 (1967).

Manuscript received March 2, 1979; revision received June 8, and accepted June 15, 1979.

Electroforced Sedimentation of Thick Clay Suspensions in Consolidation Region

MOMPEI SHIRATO
TSUTOMU ARAGAKI
AKIRA MANABE
Department of Chemical Engineering
Nagoya University, Chikusa, Nagoya, Japan
and
NOBUHIKO TAKEUCHI
Department of Chemical Engineering
Hiroshima University, Senda-cho, Hiroshima, Japan

It is shown that the slow settling rates of thickened Gairome clay slurries, when initial concentrations are sufficiently concentrated for settling due to the so-called consolidation mechanism from the beginning of settling, can be greatly enhanced by application of D.C. voltages. Equations for settling due to the consolidation mechanism are developed in view of the influence of the gravitational and the applied electric field. It is demonstrated that the settling rates increase remarkably with increasing electric field intensity. The settling rates and the porosity distributions in settling sediments calculated by the new equations compare favorably with experimental observations.

SCOPE

It has long been known that a charged region, called the electric double layer, appears at the interface between a suspended particle and the surrounding water. In an external D.C. electric field, the presence of the electric double layer causes effects on particle and liquid motion that are generally known as electrokinetic phenomena. Only a few industrial applications of these phenomena have been found, mainly in water clarification, cake and soil dehydration, and refining of natural clays. The works by Moulik et al. (1967) and Yukawa et al. (1971, 1972) imply a possibility of applications in filtering hard to filter materials such as bentonite clay and colloidal suspensions.

The present study is concerned with sedimentation due to consolidation of highly concentrated suspensions in D.C. electric fields. Its main objectives are to make clear the effects of electric fields on settling rates experimentally and to develop a basic mathematical method for analyzing electroforced settling behavior.

CONCLUSIONS AND SIGNIFICANCE

Sedimentation processes of highly concentrated slurries have been widely employed in sludge treatment and in the chemical and metallurgical industries. There exists a limiting slurry concentration for settling under the so-called consolidation mechanism. Settling rates due to consolidation are usually very low, and techniques for enhancing these rates could be useful.

The aggregate-floc model by Michaels and Bolger (1962) enables one to estimate the value of the limiting slurry concentration mentioned above. If the initial concentration of suspension is higher than the internal solid concentration of aggregates, only flocs, resulting from the perfect collapse of all aggregates, can exist in the suspension. Consequently, consolidation will occur from the beginning of sedimentation. In accordance with Michaels and Bolger's concept, preliminary settling experiments were carried out for Mitsukuri Gairome clay deionized water suspensions, and with the aid of a modified form of Richardson and Zaki's equation (Richardson and Zaki, 1954; Shirato et al., 1970), the limiting solid concentration was determined as

0001-1541-79-2759-0855-$01.05. © The American Institute of Chemical Engineers, 1979.

3.44 vol% for the suspension used in this study. Compression-permeability characteristics of suspended solids at low compressive pressures, which play an important role as a basic tool for investigating the internal structures of settling sediments, are obtained by settling experiments (Shirato et al., 1970).

Settling experiments were conducted under the applications of various D.C. voltages. It has become apparent that the settling rates of sediments increase remarkably with increasing intensity of electric field, as illustrated in Figures 8*a* and *b*, and electroforced sedimentation may be useful especially for low settling rate suspensions of extremely fine or colloidal materials.

The settling of concentrated slurries in electric fields is mathematically analyzed in view of the internal flow mechanism through sediments, and an electroforced consolidation Equation (13) is presented. The equation is made valid for conventional, gravitational sedimentation due to consolidation by setting the intensity of the electric field E at 0.

On the basis of compression-permeability data, time changes in both sediment height and internal structure of settling sediments in electric fields are calculated by integrating Equation (13) numerically. The calculated results coincide fairly well with experiments when E is not larger than about 30 v/m.

From measurement of internal porosity distributions in the sediments, it becomes apparent that an abnormally strong consolidation takes place in the upper portions of the settling sediments when E somewhat exceeds 30. It has also been shown experimentally that for cases where E is much larger than 30, a remarkable decrease in electric potential occurs at the surface layers, and the strong consolidation in the upper portions may be consistent with the abnormal potential distribution.

ANALYSIS

Fundamental concepts of the so-called consolidation theory in soil mechanics developed by Terzaghi (Terzaghi and Peck, 1948) have played a significant role in various dehydration problems (Shirato et al., 1970; Yagi and Yamazaki, 1960; Mikasa, 1967; Blake and Colombera, 1977; Körmendy, 1964). To investigate the internal mechanism of sedimentation due to consolidation under a D.C. electric field, a modification of Terzaghi's theory has been used.

Basic Consolidation Equations for Electro Forced Sedimentation

The gravitational and electrokinetic forces acting on particles in sediments yield the excess hydraulic pressure p_L, and the gradient of p_L causes an upward liquid flow through the porous media, resulting in compaction of the sediments. As a variable for indicating an arbitrary position in settling sediments, it is convenient to use the solid volume ω per unit cross-sectional area of settling cylinder measured from the bottom of the sediments.

Apparent liquid velocity relative to solids u can be written as

$$u = -\frac{1}{\mu\alpha\rho_s}\cdot\frac{\partial p_L}{\partial \omega} \tag{1}$$

The local specific resistance α may be related to the effective specific surface S_0 and the porosity ϵ by Kozeny's equation:

$$\alpha \equiv \frac{kS_0^2(1-\epsilon)}{\rho_s\epsilon^3} \tag{2}$$

In Equation (1), u is directed upward and is consistent with the positive direction of the ω axis.

The basic differential equation relating the change in u to the change in void ratio e can be obtained from a mass balance of fluid with respect to a volume element $d\omega$ in the sediment:

$$\frac{\partial u}{\partial \omega} = -\frac{\partial e}{\partial \theta} \tag{3}$$

Here e is defined by

$$e \equiv \frac{\epsilon}{1-\epsilon} \tag{4}$$

To investigate the internal mechanism of settling sediments, the relation between excess hydraulic pressure p_L and solid compressive pressure p_s is needed. In cake filtration, Tiller (1953), Collins (1963), and Shirato and Aragaki (1969) have theoretically derived the $p_L - p_s$ relation by considering the balance of forces acting on a differential thickness in filter cake. The same procedure can be applied to electroforced sedimentation due to consolidation.

Under the influence of an external electric field, the presence of an electric double layer produces an electrokinetic force on the surface of the solid particle and also a force on the liquid layer in the opposite direction. Because the latter force acts only on the liquid layer in the vicinity of the solid surface and not on the remaining part of the liquid, and because the flow path of the liquid is extremely tortuous, it may be supposed that this force contributes only to the possible convection of liquid in small pore spaces and, perhaps, not substantially to the compaction of sediment. For simplicity, this force is assumed, as a first approximation, to be negligible.

The electroforced sedimentation of highly concentrated suspensions may proceed under the influence of four kinds of forces, that is, the electro-kinetic force acting on solids, the gravitational force, the excess hydraulic pressure, and the solid compressive pressure, as shown in Figure 1. The $p_L - p_s$ relation can be determined by taking the balance of the forces exerted on a differential volume element $d\omega$ as

$$\left(\frac{\partial p_L}{\partial \omega} + \frac{\partial p_s}{\partial \omega}\right) = -\{(\rho_s - \rho)g + F\} \tag{5}$$

where F can be easily described in terms of the double layer thickness δ and the zeta potential ζ. Suppose that a particle of volume v_p and surface area S_p is placed in an external electric field E. If the size of the particle is much larger than δ, the particle surface can be considered always as a plane, and the electric charge per particle Q_p may be expressed with sufficient accuracy by the following equation for a plane condenser:

$$Q_p = \frac{\zeta D S_p}{\delta}$$

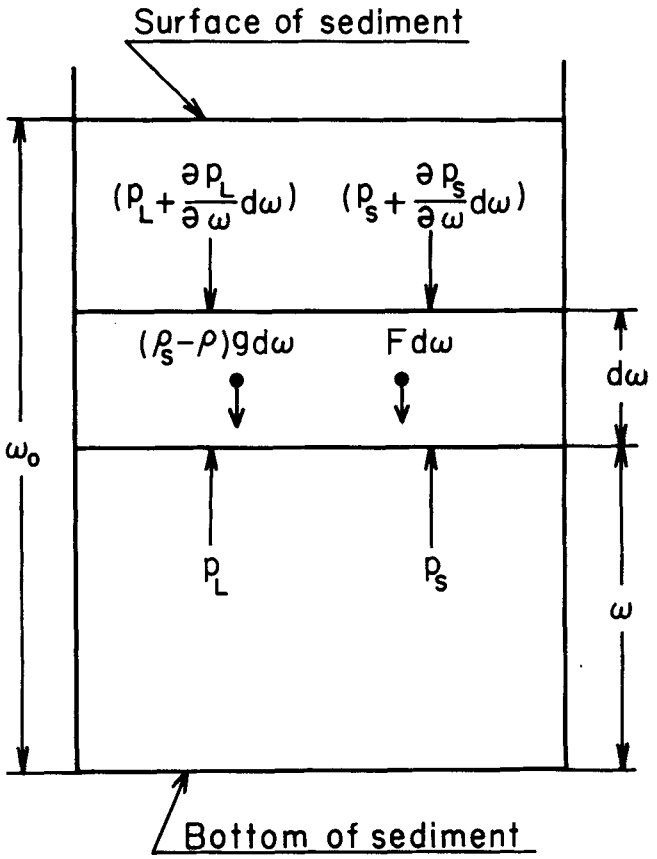

Figure 1. Forces acting on an element $d\omega$.

The number of particles per cubic meter net solid volume is $1/v_p$, and the charge Q per unit volume of solids is given by

$$Q = Q_p \cdot (1/v_p) = \frac{\zeta D S_p}{\delta v_p} \tag{6}$$

Then the electrokinetic force per unit solid volume F can be represented by

$$F = Q \cdot E = \frac{\zeta D S_0 E}{\delta} \tag{7}$$

In Equation (7), S_p/v_p is replaced by the effective specific surface of solids S_0. The value of k in Equation (2), frequently taken as 5 for incompressible cakes, may vary for compressible sediments. If the value of k is, as a first approximation, assumed constant, the effective specific surface surface S_0 may be dependent on porosity (Grace, 1953), and consequently F may vary through the settling sediments.

For simplicity, the apparent specific weight of the solids Γ, in which both the gravitational and the electrokinetic forces are considered together, is introduced as

$$\Gamma \equiv (\rho_s - \rho)g + F \tag{8}$$

Combining Equation (1) with Equations (5) and (8), we get

$$u = \frac{1}{\mu\rho_s} \cdot \frac{1}{\alpha}\left(\Gamma + \frac{\partial p_s}{\partial \omega}\right) \tag{9}$$

and substituting the above equation into Equation (3), we get

$$\frac{\partial^2 p_s}{\partial \omega^2} - \frac{1}{\alpha}\frac{d\alpha}{dp_s}\left\{\left(\Gamma - \alpha\frac{d\Gamma}{d\alpha}\right) + \frac{\partial p_s}{\partial \omega}\right\}\frac{\partial p_s}{\partial \omega} = \mu\rho_s\alpha\left(-\frac{de}{dp_s}\right)\cdot\frac{\partial p_s}{\partial \theta} \tag{10}$$

where it is assumed that both e and α are functions of p_s alone. Boundary and initial conditions may be described as

$$\frac{\partial p_s}{\partial \omega} = -\Gamma \quad \text{at} \quad \omega = 0 \tag{11a}$$

$$p_s = p_0^* \quad \text{at} \quad \omega = \omega_0 \tag{11b}$$

$$p_s = p_0 \quad \text{at} \quad \theta = 0 \tag{11c}$$

Equation (11a) is equivalent to the impermeable bottom condition, that is, $\partial p_L/\partial \omega = 0$ as is apparent from Equations (5) and (8). Equation (11c) indicates batch sedimentation of a thickened slurry whose concentration is initially uniform throughout its height. At the interfacial surface of settling sediments, it can be assumed that no compaction takes place, and the surface porosity may be constant during the sedimentation process and equal to the initial porosity of the original suspension. One can, therefore, assume that $p_s = p_0^* = p_0$ at the surface of the sediment where $\omega = \omega_0$. p_0 denotes the value of p_s corresponding to the initial concentration of the suspension and can be determined by the $\epsilon - p_s$ data. It should be noted that the assumption, that is, $p_s = p_0^* = p_0$, is valid under the limiting condition $E \lesssim 30$. When E is much larger than 30, experimental results show that some compaction takes place also in the upper portion of the sediments, and p_0^* is not equal to p_0.

Equation (10) shows very poor convergence in its numerical integration, especially at the initial stage of settling. To overcome this difficulty, the following dimensionless variables have been introduced:

$$\phi \equiv \frac{1}{\omega_0}\int_{p_0}^{p_s}\frac{1}{\Gamma}\,dp_s \tag{12a}$$

$$\xi \equiv \omega/\omega_0 \tag{12b}$$

$$T \equiv \theta/\theta_0 \tag{12c}$$

Using the new variables, Equations (10) and (11) are rewritten in dimensionless form as

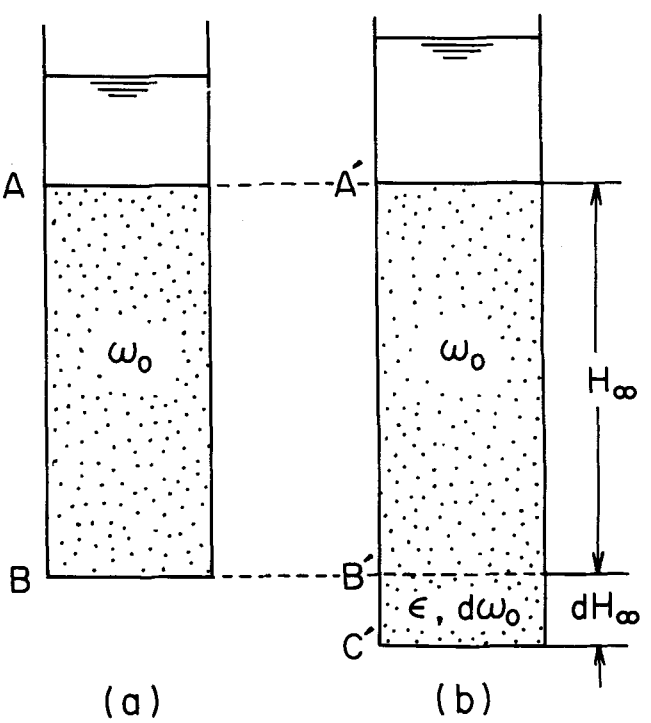

Figure 2. Schematic diagram of final equilibrium height and solid volume per unit area.

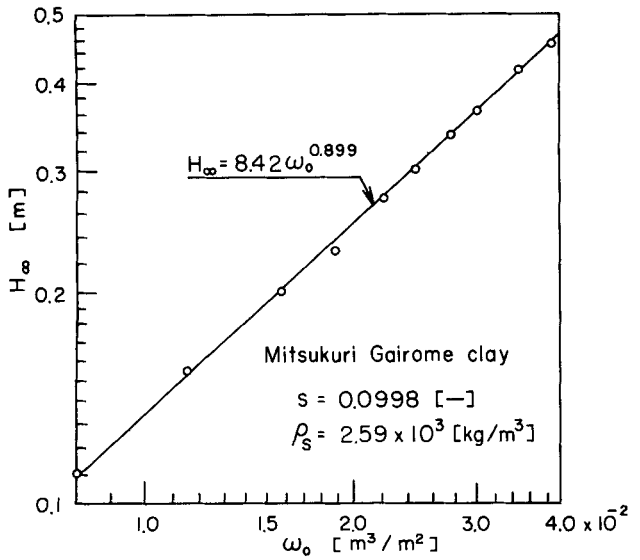

Figure 3. Logarithmic plot of H_∞ vs. ω_0.

$$\frac{\partial \phi}{\partial T} = C_1 \frac{\partial^2 \phi}{\partial \xi^2} - C_1 C_2 \cdot \left(1 + \frac{\partial \phi}{\partial \xi}\right) \frac{\partial \phi}{\partial \xi} \tag{13}$$

and

$$\frac{\partial \phi}{\partial \xi} = -1 \quad \text{at} \quad \xi = 0 \tag{14a}$$

$$\phi = 0 \quad \text{at} \quad \xi = 1 \tag{14b}$$

$$\phi = 0 \quad \text{at} \quad T = 0 \tag{14c}$$

where C_1 and C_2 are defined by

$$C_1 \equiv \frac{\theta_0}{\mu \rho_s \omega_0^2 \alpha}\left(-\frac{dp_s}{de}\right)$$

$$C_2 \equiv \frac{\omega_0}{\alpha}\frac{d\alpha}{dp_s}\left(\Gamma - \alpha \frac{d\Gamma}{d\alpha}\right) \tag{15}$$

To solve Equation (13), numerical calculations based upon the Runge-Kutta-Gill method were made by using an electronic computer (FACOM 230-75 at Nagoya University Computation Center).

Compression Permeability Characteristics of Suspended Solids

The compression-permeability cell method (Grace, 1953; Tiller, 1953, 1955; Okamura and Shirato, 1955) has long served as a basic tool for research in cake filtration and expression. This method, however, is not adequate for sedimentation analysis, as it cannot cover the range of relatively low solid compressive pressures encountered in sedimentation analysis. In this study, compression-permeability characteristics of suspended solids are determined by using an alternative method presented by Shirato et al. (1970).

Compression Characteristics

Suppose that a suspension containing net solid volume per unit area ω_0 settles in a vertical container as shown in Figure 2*a*, and let H_∞ be the final equilibrium height of sediment. If the initial volume of the suspension is increased by the volume $d\omega_0$, the final height of the sediment will become $(H_\infty + dH_\infty)$, as shown in Figure 2*b*. The total sediment AB in Figure 2*a* must be identical to the partial sediment A′B′ in Figure 2*b*, and consequently the solid volume in the part B′C′ may be $d\omega_0$. Denoting the thickness and the porosity of the part B′C′ as dH_∞ and ϵ, respectively, one can obtain the following relations:

$$\epsilon = 1 - \frac{d\omega_0}{dH_\infty} \tag{16}$$

$$p_s = (\rho_s - \rho) g \omega_0 \tag{17}$$

It is assumed that the side wall friction between the solids and the container wall is negligible.

In accordance with previous work (Shirato et al., 1970), plots of the experimental $H_\infty - \omega_0$ relation gives a linear relation on log-log paper, and the following empirical equation can be obtained:

$$H_\infty = a\omega_0^b \tag{18}$$

Substituting Equation (18) into Equation (16) and eliminating ω_0 with the aid of Equation (17), we get

$$\epsilon = 1 - B p_s^\beta \tag{19}$$

where

$$B \equiv \frac{1}{ab\{(\rho_s - \rho)g\}^{1-b}}, \quad \beta \equiv 1 - b \tag{20}$$

Settling experiments were carried out for various initial heights of 4.11 vol % Mitsukuri-Gairome Clay suspension, and the final equilibrium heights H_∞ vs. ω_0 are shown in Figure 3. The straight line in the figure indicates that $a = 8.42$ and $b = 0.899$, and therefore $B = 0.0498$ and $\beta = 0.101$. These empirical values in Equation (19) may not be valid for very low values of p_s.

Permeability Characteristics

Initial settling velocity of sediment surface v_0 in the gravitational field may be used to determine the permeability characteristics of the solids. At the beginning of settling of a uniform solid-liquid mixture, p_s equals a constant p_0 at any position in the sediment, and it becomes apparent from Equation (5) that the initial gradient of p_L satisfies the following equation:

$$-\left(\frac{\partial p_L}{\partial \omega}\right)_0 = (\rho_s - \rho) g \tag{21}$$

A combination of Equations (1) and (2) with Equation (21) yields a relation between v_0 and kS_0^2 for a thickened suspension of initial porosity ϵ in the form

$$kS_0^2 = \frac{\epsilon^3 (\rho_s - \rho) g}{\mu v_0 (1 - \epsilon)} \tag{22}$$

Figure 4 shows the values of kS_0^2 determined by using Equation (22) and experimental v_0 values of various

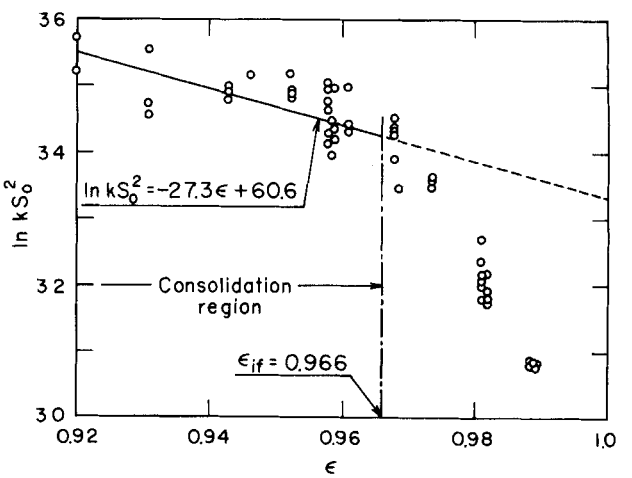

Figure 4. Permeability characteristic.

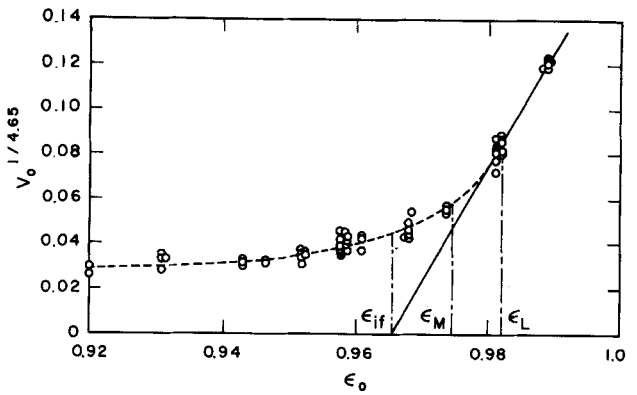

Figure 5. $v_0^{1/4.65}$ vs. ϵ_0.

initial concentrations. In the figure, ϵ_{if} denotes the limiting porosity. Provided the value of the initial suspension porosity is smaller than ϵ_{if}, compaction of settling sediment will take place from the beginning of the sedimentation process. The suspensions utilized in this study are confined to the region of initial porosities smaller than ϵ_{if}, and the experimental results of kS_0^2 in that region, as shown in the figure, may be approximately expressed by

$$kS_0^2 = C \exp\{b^*(\epsilon_{if} - \epsilon)\} \qquad (23)$$

where $b^* = 27.3$ [−] and $C = 7.41 \times 10^{14}$ for Mitsukuri-Gairome Clay suspensions.

Limiting Porosity

In their valuable contributions to sedimentation analysis for flocculated suspension, Michaels and Bolger (1962) postulated a structural model which assumes that basic flow units are small clusters of particles called flocs, and that these flocs group into clusters of flocs called aggregates. They suggested an interesting method for estimating the mean size and the internal solid concentration of the aggregates by using a modified Richardson and Zaki equation (Richardson and Zaki, 1954).

Sedimentation behavior is classified into three types according to the initial concentration range of suspensions. Gotoh et al. (1968) and Shirato et al. (1970) determined the limiting concentrations for the regions of these three types of behavior with the aid of Equation (24), which relates the initial settling velocity v_0 to the initial porosity ϵ_0 of the original suspension, the average equivalent spherical diameter d_f of aggregates, and its internal porosity ϵ_{if}:

$$v_0^{1/4.65} = \left\{ \frac{g d_f^2 (\rho_s - \rho)}{18\mu(1 - \epsilon_{if})^{3.65}} \right\}^{1/4.65} (\epsilon_0 - \epsilon_{if}) \qquad (24)$$

The above equation is essentially identical with that presented by Michaels and Bolger (1962). As far as the low concentration (that is, high porosity) region is concerned, the plots of the experimental data of $v_0^{1/4.65}$ vs. ϵ_0 result in a straight line, as shown in Figure 5. The abscissa intercept and the slope of the straight line yield the values of $\epsilon_{if} = 0.966$ and $d_f = 1.05 \times 10^{-2}$ cm for Mitsukuri-Gairome Clay suspensions.

The porosities ϵ_L and ϵ_M in the figure correspond to porosities of the original suspensions equivalent to the loosest packing and the closest packing of aggregates, respectively. In the dilute concentration region ($\epsilon_0 > \epsilon_L$), free or hindered settling may take place. In the intermediate concentration region ($\epsilon_{if} < \epsilon_0 < \epsilon_M$), sedimentation behavior becomes unstable owing to partial collapse of aggregates. In the higher concentration region ($\epsilon_0 < \epsilon_{if}$), no aggregate can exist, compaction takes place from the beginning of sedimentation, and settling behavior becomes comparatively reproducible. It should be noted that Equation (13) is valid only for the suspensions of initial porosity lower than ϵ_{if}.

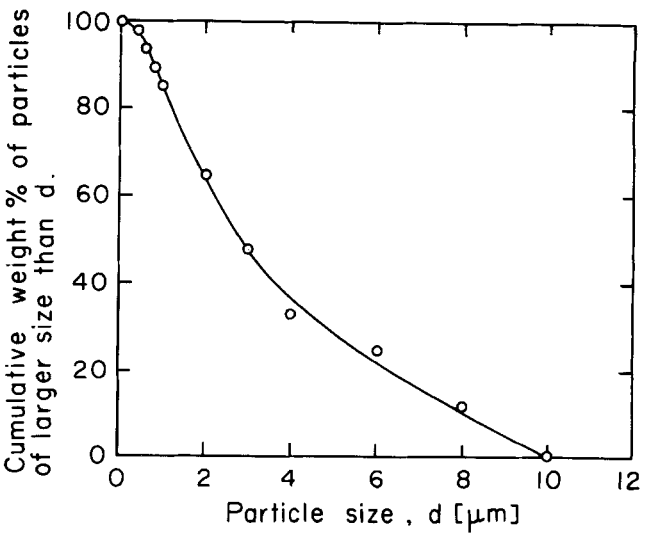

Figure 6. Particle size distribution determined by a light-transmission method combined with sedimentation.

SEDIMENTATION EXPERIMENTS UNDER ELECTRIC FIELDS

Experimental Apparatus and Procedure

The apparatus used for the sedimentation experiments consisted of a Plexiglas cylinder of 5.0 cm inside diameter* and a pair of top and bottom brass disk electrodes. The top electrode disk is perforated so that the small amount of gas created by electrolysis can be removed. Solid material used in this study was Mituskuri-Gairome Clay ($\rho_s = 2.59 \times 10^3$ kg/m^3), the particle size distribution being shown in Figure 6.

The clay deionized water suspensions were prepared in the higher concentration region where the initial porosity does not exceed ϵ_{if}, that is, 0.966. To attain sufficient formation of flocs, the suspension in a beaker was agitated for about 30 min by a stirrer. Air bubbles were removed by using a vacuum pump for 5 min, and then the suspension was carefully poured into a settling cylinder in a temperature controlled chamber. The position of the top electrode was adjusted to contact with the surface of the suspension, and a constant D.C. voltage was applied.

Under conditions of various initial heights H_0, initial porosities ϵ_0, and D.C. voltages, sedimentation experiments were carried out; the heights of the settling sediments H were measured with the lapse of the time θ by using a scale fixed to the cylinder or by an autocathetometer where necessary. After 60, 120, and 180 min, sedimentation experiments were stopped, and porosity distributions in sediments were measured by weighing.

Electric potential distributions through settling sediments were measured by using the apparatus shown in Figure 7. The cylinder wall was provided with fourteen pin type of electrodes (0.5 mm diameter platinum pins) arranged in a helical pattern up the wall. Electric potentials based on the reference electrode shown in Figure 7 were measured.

RESULTS AND DISCUSSION

In Figures 8*a* and *b*, the experimental results of normalized sediment height H/H_0 vs. time θ for various electric field intensities E, that is, the applied voltage divided by the distance between electrodes, are shown. Settling

Gotoh et al. (1968) indicated that where the diameter of a Plexiglas cylinder exceeds about 5 cm, the effect of side wall friction on settling behavior can be neglected.

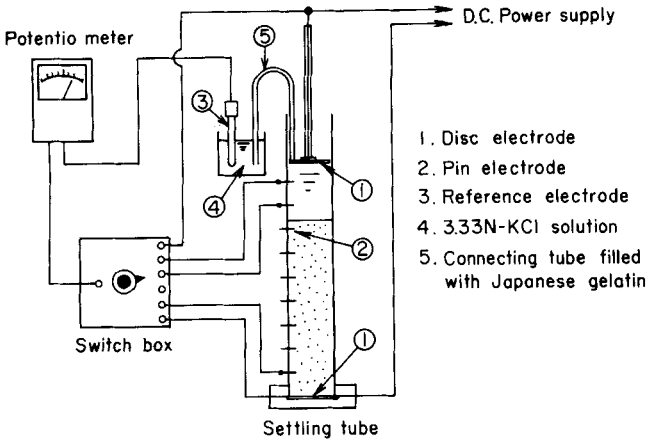

Figure 7. Apparatus for measuring electric potential distribution in settling sediment.

velocities increase remarkably with increasing field intensity. It can be seen from the figures that the lower the initial height the stronger the electrokinetic effect. The remarkable enhancement of settling velocity suggests the possible application of electroforced sedimentation to separations of solid-liquid mixtures of extremely low settling velocities. The maximum electric current observed in this study was only 3.0 mA.

Porosity distributions in the sediments were determined after a lapse of 180 min from the beginning of sedimentation experiments and are illustrated in Figure 9 for various E values. Except for the case where $E = 30.2$, remarkable compactions are observed in not only the bottom layers but also the upper portions of the settling sediments. Variations of porosity distribution with time are shown in Figure 10 for the case where $E = 124$, $H_0 = 0.16$ m, and $\epsilon_0 = 0.942$. Compaction in the upper portion has a significant effect on settling velocity.

Variations of electric potential distribution in the settling sediments were determined by using the apparatus shown in Figure 7, and the experimental results are shown in Figure 11. The dotted lines in the figure indicate the sediment surfaces at various times. At the interfacial surface layer of the sediment, the electric potential decreases very steeply, as seen from the figure. Consequently, the electric field intensity at the surface layer becomes much stronger, and a stronger electrokinetic force may act on the solid particles in the surface layer and results in a remarkable compaction of the upper portion of the sediment, as shown in Figures 9 and 10. Strict analysis

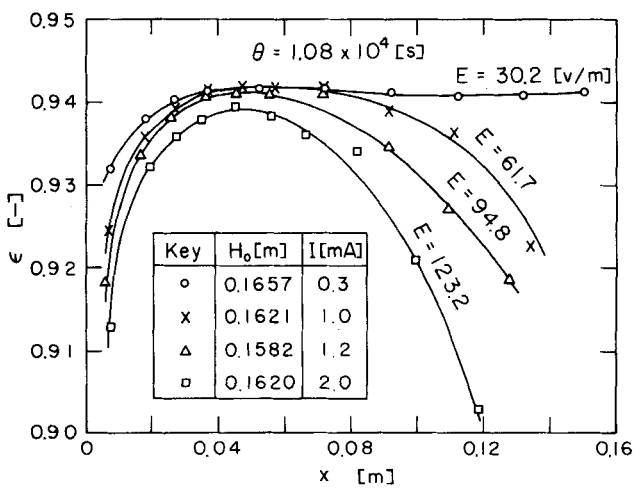

Figure 9. Effect of applied field intensity E on porosity distribution.

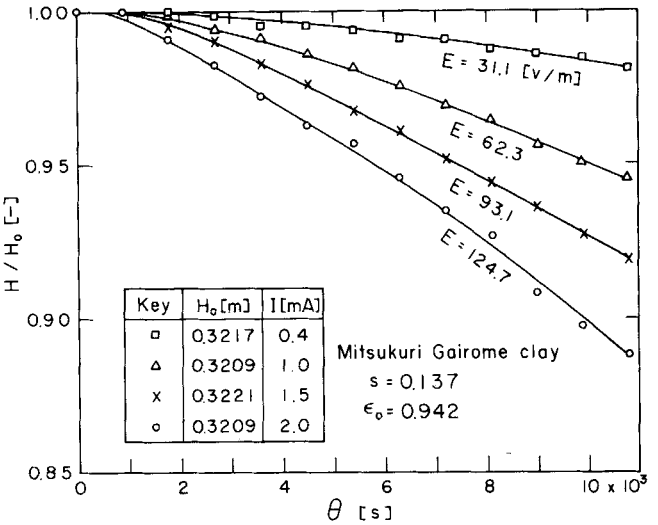

Figure 8a. Variations of sediment heights ($H_0 \doteqdot 0.32$ m).

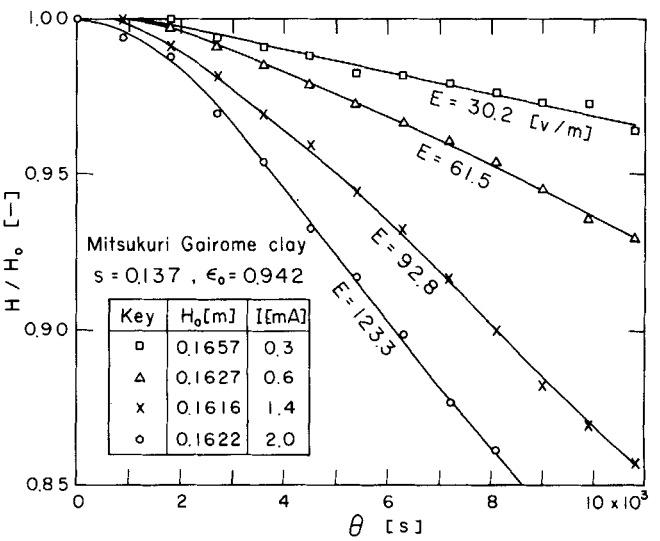

Figure 8b. Variations of sediment heights ($H_0 \doteqdot 0.16$ m).

of such a phenomenon, however, necessitates further theoretical and experimental work.

Theoretical predictions based upon Equation (10) are made for the cases where $E \lesssim 30$, that is, under conditions where surface compaction does not take place. Now, p_0^* can be replaced by p_0, and the problem may be reduced to Equations (13) and (14).

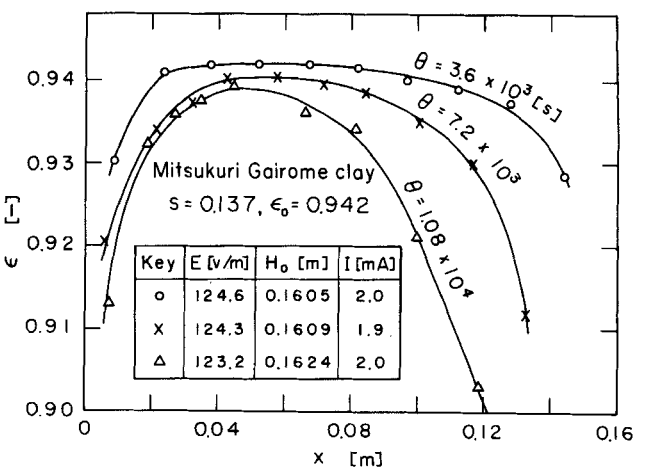

Figure 10. Time variation of porosity distribution.

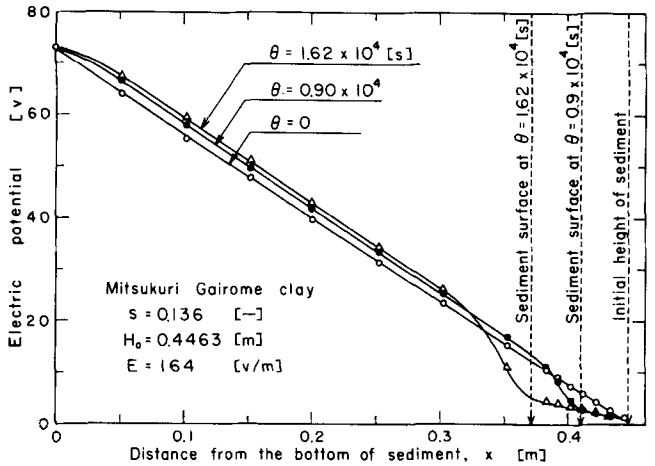

Figure 11. Electric potential distribution through a settling sediment.

To carry out numerical integrations of Equation (13), one has to determine three characteristic values concerning the so-called electric double layer, that is, its Zeta potential, its thickness, and the dielectric constant of the liquid. Fortunately, these values always appear in grouped form as $\zeta D/\delta$, as may be seen from Equation (7), which can be evaluated by the following fitting method. By using several presumed values of $\zeta D/\delta$, the theoretical H/H_0 vs. θ relations calculated from Equations (13) and (14) are compared with an experimental result. As may be seen from Figure 12, the theory shows good agreement with experiment when $\zeta D/\delta = 0.513 \times 10^{-4}$ vF/m². As a first approximation, it is assumed that $\zeta D/\delta$ may be a constant equal to 0.513×10^{-4} for all experimental runs of the same suspensions of equal concentration when $E \lesssim 30$. On the assumption that $\zeta D/\delta = 0.513 \times 10^{-4}$, theoretical calculations of both the variations of sediment height and internal porosity distribution in settling sediment compare fairly well with experiment in Figures 13 and 14, respectively.

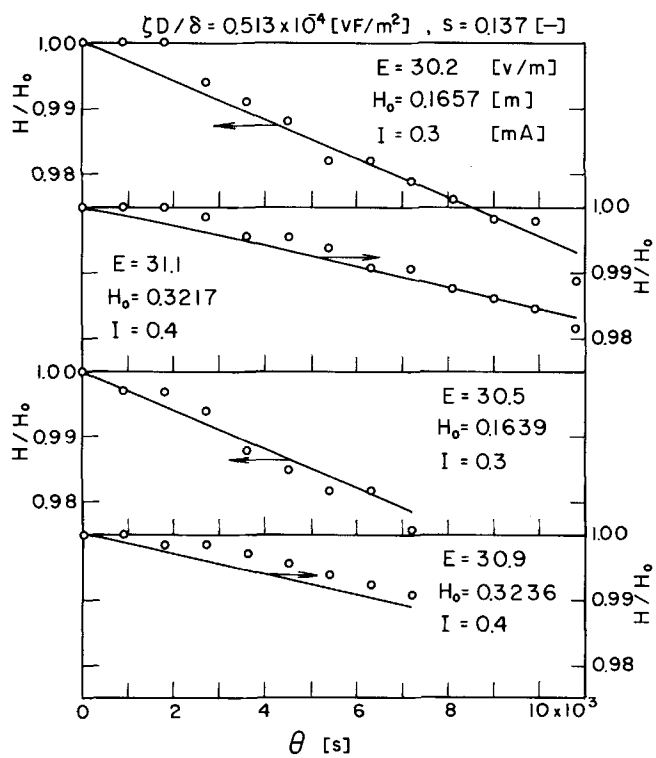

Figure 13. Calculated and experimental values of H/H_0 vs. θ for the cases where $s = 0.137$.

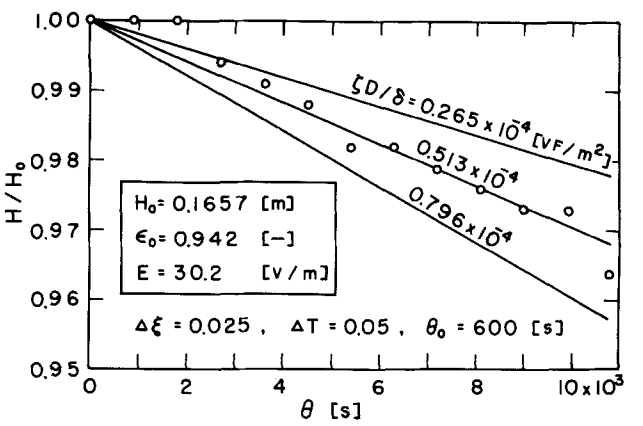

Figure 12. Determination of $\zeta D/\delta$ by fitting method.

For a suspension of higher concentration (that is, $\epsilon_0 = 0.903$), the fitting method gives 1.77×10^{-4} as the value of $\zeta D/\delta$, and the results are shown in Figure 15.

It is interesting to note that the $\zeta D/\delta$ value of a suspension changes with its initial concentration. This may imply that the characteristics of the electric double layer may vary when sediment compaction proceeds and may not be constant through the sediment, a condition that conflicts with the rough assumption assumed in this study. Provided the mechanism of $\zeta D/\delta$ becomes clearer, more rigorous calculations can be made for wider ranges of concentration.

CONCLUSION

The consolidation mechanism in settling processes of electroforced sedimentation for highly concentrated suspensions is mathematically analyzed in view of the internal flow mechanism of the fluid. A consolidation Equation (13) of partial differential form and a force balance Equation (5) which gives the relation among the solid compressive pressure p_s, the excess hydraulic pressure p_L, and the electrokinetic force F are newly derived. By setting E and F at 0, the equations reduce to the usual

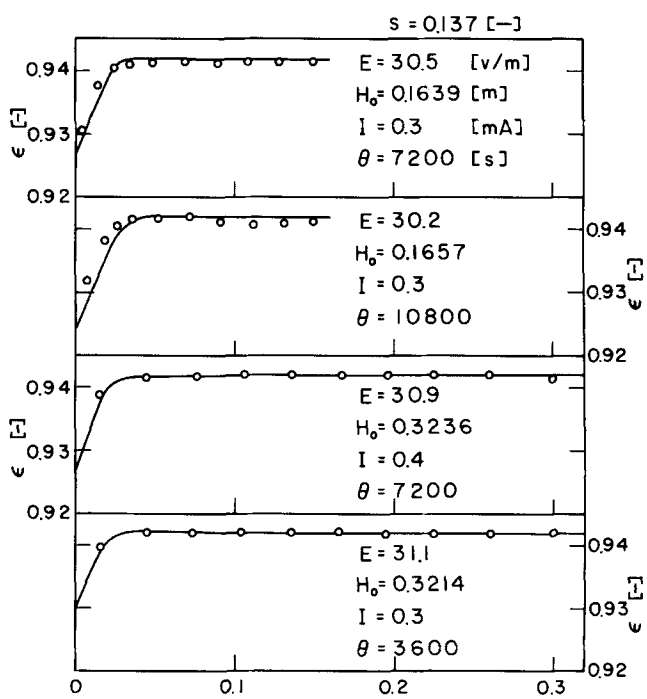

Figure 14. Comparison of experimental and calculated porosity variations for the cases where $s = 0.137$.

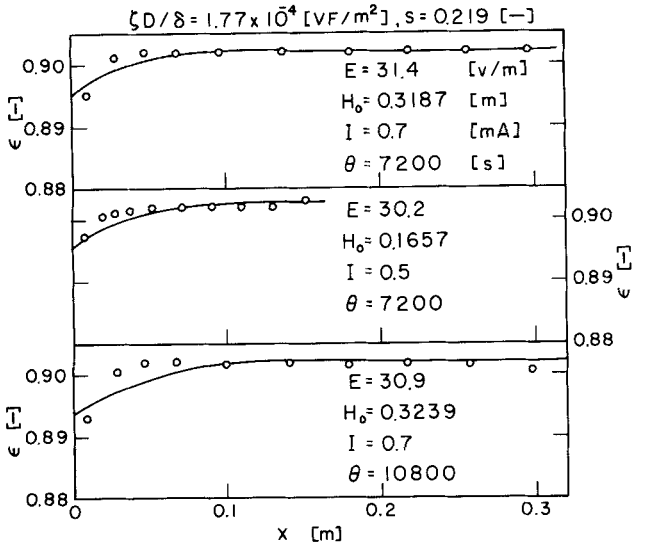

Figure 15. Porosity distributions for the case where $s = 0.219$.

equations of gravitational sedimentation due to consolidation.

For highly concentrated slurries of Mitsukuri-Gairome Clay-water suspensions, electroforced sedimentation experiments were carried out under various electric field intensities E. It has become apparent that the settling rates of sediments increase remarkably with increasing E. Remarkable enhancement in settling velocities may suggest possible industrial application of electroforced sedimentation.

On the basis of the compression-permeability data determined by a settling method, numerical integrations of Equation (13) were performed under various conditions. Fairly good agreement between theory and experiment is shown for cases where $E \lesssim 30$. In addition, it was found experimentally that when $E \gtrsim 30$, consolidation of the upper portions of settling sediments does occur and that electric potential distributions show a steep decrease at the surface layers of settling sediments.

ACKNOWLEDGMENT

The authors wish to acknowledge the valuable assistance rendered by Shin Fukushima, Kōji Okumura, and Toshio Teramoto.

NOTATION

a = empirical constant, m^{1-b}
b = empirical constant
b^* = empirical constant
B = empirical constant, $(N/m^2)^{-\beta}$
C = empirical constant, $1/m^2$
d_f = mean diameter of aggregate, cm
D = dielectric constant, F/m
e = local void ratio
E = intensity of electric field, that is, the applied voltage divided by the distance between electrodes, v/m
F = electrokinetic force acting on unit volume of solids, N/m^3
g = gravitational acceleration, m/s^2
H = height of settling sediment, m
H_0 = initial height of sediment, m
H_∞ = final equilibrium height of sediment, m
k = Kozeny constant
p_L = local hydraulic pressure, N/m^2
p_s = local solid compressive pressure, N/m^2
p_0 = p_s value corresponding to initial porosity, N/m^2
p_0^* = p_s value at the interfacial surface of sediment, N/m^2
Q = electric charge per unit volume of solids, C/m^3
Q_p = electric charge per particle, C
s = mass fraction of solids in slurry
S_p = surface area of one particle, m^2
S_0 = specific surface area of particles, m^2/m^3
T = dimensionless time defined by Equation (12c)
u = apparent liquid velocity relative to solids, m/s
v_0 = initial settling velocity of surface of sediment, m/s
v_p = volume of one particle, m^3
x = distance measured from the bottom of sediment, m

Greek Letters

α = local specific resistance, m/kg
β = empirical constant
Γ = apparent specific weight of solids defined by Equation (8), N/m^3
δ = thickness of electric double layer, m
ϵ = local porosity
ϵ_{if} = internal porosity of aggregates
ϵ_L = porosity of original suspension equivalent to the loosest packing of aggregates
ϵ_M = porosity of original suspension equivalent to the closest packing of aggregates
ϵ_0 = initial porosity
ζ = zeta potential, V
θ = settling time, s
θ_0 = proper time for normalization, s
μ = viscosity, kg/m s
ξ = modified dimensionless distance expressed in solids fraction as defined by Equation (12b)
ρ = density of liquid, kg/m^3
ρ_s = density of solids, kg/m^3
ϕ = local value of reduced solid compressive pressure defined by Equation (12a)
ω = variable for representing an arbitrary position in sediment, that is, volume of solids per unit cross-sectional area measured from the bottom of sediment, m
ω_0 = total volume of solids per unit cross-sectional area, m

LITERATURE CITED

Blake, J. R., and P. M. Colombera, "Sedimentation: a Comparison between Theory and Experiment," *Chem. Eng. Sci.*, **32**, 221 (1977).

Collins, R. E., *Modern Chemical Engineering*, Vol. 1, "Physical Operations," p. 327-330, Reinhold, New York (1963).

Gotoh, K., T. Sakai, H. Kato, and M. Shirato, "Sedimentation of Flocculated Slurry," *Kagaku Kogaku*, **32**, 1105 (1968).

Grace, H. P., "Resistance and Compressibility of Filter Cakes," *Chem. Eng. Progr.*, **49**, 303, 367 (1953).

Körmendy, I., "A Pressing Theory with Validating Experiments on Apples," *J. Food Sci.*, **29**, 631 (1964).

Michaels, A. S., and J. C. Bolger, "Settling Rates and Sediment Volumes of Flocculated Kaolin Suspensions," *Ind. Eng. Chem. Fundamentals*, **1**, 24 (1962).

Mikasa, M., "The Consolidation of Soft Clay—A New Consolidation Theory and its Application," *Kashima Shuppan Kai* (1967).

Moulik, S. P., F. C. Cooper, and M. Bier, "Forced-Flow Electrophoretic Filtration of Clay Suspensions—Filtration in an Electric Field," *J. Colloid Interface Sci.*, **24**, 427 (1967).

Okamura, S., and M. Shirato, "P_x-distribution within Cakes in Compression-Permeability Experiments (about Ignition-plug Slurry)," *Kagaku Kogaku*, **19**, 111 (1955).

Richardson, J. F., and W. N. Zaki, "Sedimentation and Fluidisation: Part I," *Trans. Inst. Chem. Eng.*, **32**, 35 (1954).

Shirato, M., and T. Aragaki, "The Relations between Hydraulic and Compressive Pressures in Non Uni-Dimensional Filter Cakes," *Kagaku Kogaku*, 33, 205 (1969).
Shirato, M., H. Kato, K. Kobayashi, and H. Sakazaki, "Analysis of Settling of Thick Slurries due to Consolidation," *J. Chem. Eng. Japan*, 3, 98 (1970).
Terzaghi, K., and R. B. Peck, *Soil Mechanics in Engineering Practice*, p. 233-242, Wiley, New York (1948).
Tiller, F. M., "The Role of Porosity in Filtration," *Chem. Eng. Progr.*, 49, 467 (1953); 51, 282 (1955).
Yagi, S., and Y. Yamazaki, "Fundamental Studies on Settling of Suspensions," *Kagaku Kogaku*, 24, 81 (1960).
Yukawa, H., H. Chigira, T. Hoshino, and M. Iwata, "Fundamental Study of Electroosmotic Filtration—Effect of Strength of Electric Field on Flow Rate of Permeation," *J. Chem. Eng. Japan*, 4, 370 (1971).
Yukawa, H., "The Effects of Electrophoresis and Electroosmosis on Rate of Filtration and Sedimentation," Part I, p. 70-79, Proc., First Pacific Chemical Engineering Congress, Kyoto, Japan (1972).

Manuscript received August 14, 1978; revision received April 3, and accepted April 20, 1979.

The Growth of Competing Microbial Populations in a CSTR With Periodically Varying Inputs

GREGORY STEPHANOPOULOS
A. G. FREDRICKSON
and
RUTHERFORD ARIS
Department of Chemical Engineering and Materials Science
University of Minnesota
Minneapolis, Minnesota 55455

The operation of a periodically forced chemostat (CSTR) in which two microbial populations compete for the same nutrient has been examined. Easily implemented criteria for the stability of the resulting cycles have been obtained, using the Floquet stability theory. After examining several possibilities it was found that stable periodic trajectories of coexistence can be achieved: (a) when the dilution rate of the chemostat is properly varied in a periodic manner between two values so chosen that the growth of one population is favored by the first and the growth of the other population is favored by the second, (b) when a certain percentage of biomass and growing medium is harvested periodically from the chemostat, and (c) when both the dilution rate and the concentration of the substrate in the feed are varied simultaneously and in a periodic manner.

SCOPE

Both experiments and theories of growth show that competition of two populations for a single limiting nutrient leads to extinction of one of the populations, if they are grown in a spatially uniform environment that is subject to time-invariant external influences. This statement, or rather a less cautiously worded version of it, is known as the "competitive exclusion principle," (Hardin 1960). Its validity and applicability have been the subjects of much discussion among researchers.

Some recent theoretical work based on models that give good description of the growth of microbial populations shows that the restricted version of the competitive exclusion principle given above must be modified if more than one nutrient is limiting. Thus, Taylor and Williams (1975) suggest that n competing populations can coexist with each other if a set of at least n nutrients is limiting. Similarly, Schuelke (1976) shows that two populations could coexist if the sets of limiting nutrients for the two populations overlapped only partially. In spite of these developments, it remains true that reduction of system diversity is the usual outcome of competition in spatially uniform systems subject to time-invariant influences.

Several schemes for sustaining microbial competitors in the same environment have appeared in the literature because of the importance of competitive interaction in practical applications involving microbial activities. One of the most common is that external influences are not time invariant but that they vary so as to provide an environment in which the competitive advantage alternates between the two populations. Unfortunately, all the above schemes have been based on non-mathematical arguments and there is no assurance that a proposed scheme of time varying external influences will, in fact, allow competitors to coexist.

This study examined the effect of periodically varying inputs to coexisting competing microbial populations which grow in a continuous, well stirred vessel, usually referred to as chemostat. Criteria for the stability of the proposed cycles and examination of the effect of some operating parameters on their stability characteristics are based on Floquet stability theory. The results can be useful in establishing patterns of operation of a CSTR which can sustain the coexistence of microbial competitors and also in providing useful information about their coexistence in natural ecosystems.

Present address of the first author is: Department of Chemical Engineering, California Institute of Technology, Pasadena, California 91125.

0001-1541-79-2924-0863-$01.25. © The American Institute of Chemical Engineers, 1979.